Fabrication, modification and sensing behaviour of quartz micro/nanopipettes

Dila Kaya[a]*, Kaan Kececi[a] and Durdane Yilmaz[b]

[a]Department of Chemistry, [b]Nanoscience and Nanoengineering Program,

Istanbul Medeniyet University, 34700, Istanbul, Turkey

E-mail: dila.kaya@medeniyet.edu.tr

In this work we have used a laser-based micropipette puller system for the production of micro/nanopipettes from quartz capillaries. The pipettes were characterized via optical microscopy and SEM. We have studied the translocation events of polystyrene microparticles at different concentration and potential values to investigate the resistive-pulse sensing behaviour and performance of the obtained pipettes. We have also modified the pipette surface with (3-aminopropyl)triethoxysilane using silane chemistry in order to obtain a more neutral surface charge and promote the translocation of the particles. The modification of the pipette surface was verified using electrochemical measurements. With this purpose, current-potential (I-V) measurements were obtained and rectifications in the ionic current were investigated. The sensing of the particles was also carried out with modified pipettes which yielded longer pulse durations and higher amplitudes that improved signal to noise ratio. Furthermore, signals could be obtained at much lower potentials for modified pipettes than bare ones.

Keywords: Resistive-pulse sensing, micro/nanopipettes, surface modification.

Introduction

Resistive-pulse sensing is an established area of research that focuses on the detection and identification of molecules without labeling[1]. This method entails placing a micron or nano-sized pore between two reservoirs with electrolyte solutions and driving the particles to the oppositely charged electrodes[2]. The translocation of particles causes momentary drops in the ionic current and these signals (or events) are then used for the identification of particles. Since their first application, a variety of nanomaterials both biological and synthetic have been explored and developed to be used in a series of technologies due to their extraordinary properties[3].

Synthetic pores enable precise control over the pore size and shape, easy surface modification and integration with other systems[4]. These synthetic structures can be in the form of pores[5], channels[6] or pipettes[7] in micro/nano sizes and can be used for the detection of proteins[8], metal ions[9], DNAs[10] and nanoparticles[11].

Micro/nanopipettes are simply defined as pipettes made of capillaries with micro/nano-sized openings[7a]. The production of these pipettes are relatively easy; laser based pipette puller systems are used where capillaries are pulled from both ends and with the help of laser beams they are separated into two symmetrical micro/nano sized pipettes[12]. The geometry of the micro/nanopipette is a conical structure and this shape is similar to the conical nanopores prepared in track-etch membranes[13], which have interesting attributes for translocation phenomena[14].

Micro/nanopipettes are used in a variety of fields in science and medicine, as electrochemical or optical sensors in atomic force microscopy (AFM)[15], scanning electrochemical microscopy (SECM)[16] and many others[17], due to their small tip size, needle-like structure and easy fabrication properties. Additionally, quartz nanopipettes can be used as sensors for biomolecules such as DNA[18] or allergens[11].

In this work we have shown the resistive-pulse sensing of polystyrene microparticles functionalized with carboxyl groups (PS-COOH) using micropipettes pulled from quartz capillaries. Characterization of the pipettes was performed by optical microcopy and SEM. Translocation of PS-COOH was studied for a variety of concentration and potential values. Inner surface of the prepared pipettes were modified

with (3-aminopropyl)triethoxysilane (APTES) using silane chemistry. By taking I-V measurements and commenting on the rectification behavior of the bare and modified nanopipettes, we have verified the surface modification. The enhanced translocation was shown by the longer pulse durations and higher amplitudes obtained from modified pipettes. Also, using modified pipettes signals could be generated at lower potentials compared to the bare ones.

Experimental

Materials and methods:

Quartz capillaries (o.d.: 1.0 mm, i.d.: 0.7 mm, 10 cm) which were used in fabrication of pipettes were provided from Sutter Instruments. Laser based pipette puller (Sutter Instruments, P-2000 model) was used for the laser-assisted pulling of these capilleries. All solutions were prepared from deionized water (Millipore Direct-Q 5, Millipore Co.). Potassium chloride (KCl), (3-aminopropyl)triethoxysilane ($H_2N(CH_2)_3Si(OC_2H_5)_3$) and analytical grade ethanol (C_2H_5OH) were purchased from Sigma Aldrich. PS-COOH particles were purchased from Bangs Laboratories in the form of solid in aqueous suspension. The particles had a mean diameter of 1.05 μm and number of particles per mL solution was calculated as $1.565×10^{11}$. All chemicals were used as received without further purification. Solutions were backfilled into the micro/nanopipettes using a microfill needle.

Fabrication and characterization of the micro/nanopipettes:

Micro/nanopipettes were pulled from quartz capillaries using a lased pipette puller system. The puller has five different adjustable parameters. Designing a program with appropriate values for these settings, it is possible to prepare pipettes with desired micro/nano openings and chosen geometries. The programs for the preparation of micro/nanopipettes are given in Table 1. The tip sizes of the prepared pipettes were calculated directly from optical microscopy and SEM images.

Surface modification of micro/nanopipettes:

The previously established silane chemistry was per-

formed to modify the inner surface of the prepared pipettes[19]. Shortly, 0.2 mL of (3-aminopropyl)triethoxysilane (APTES) was added to 1 mL of ethanol and the mixture was stirred for ten minutes. Then the prepared nanopipette was backfilled with this solution and placed in pure ethanol overnight. Next day, the nanopipette was thoroughly washed with first ethanol, then di-water to remove possible residues. By using this procedure, thin silane layer was coated on the inner-surface of pipette, so the opening of the nanopipette was not blocked. The schematic representation of the modified pipette surface is given in Fig. 1.
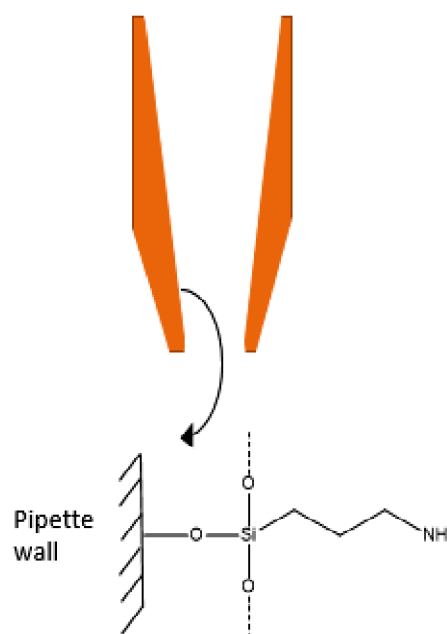

Fig. 1. Representation of the pipette surface after modification with APTES.

Current-voltage measurements:

In order to confirm that the pipette surface was indeed modified with APTES, current-voltage (I-V) measurements were performed and current rectification behaviorus were taken into account. For these measurements, bare and modified nanopipettes were backfilled with 10 or 100 mM KCl solution. One Ag/AgCl electrode was then inserted into the pipette and the other was immersed in the solution. A picoammeter/voltage source (Keithley 6487, Keithley Instruments, Cleveland, OH, USA) was used to apply transmembrane potential between –1 V and +1 V with 100 mV steps and the ionic current across the membrane was measured.

Table 1. Laser puller operating programs

Pipette opening size	Heat	Fil	Vel	Del	Pul
7 μm	700	4	55	150	50
< 200 nm	420	4	13	130	120

Resistive-pulse sensing experiments:

The pipettes were filled with 10 and 100 mM KCl solutions respectively. Then they were immersed into the same concentration of KCl solution. Ag/AgCl electrodes were used to measure the current-pulses (events). Firstly, background current measurements were recorded for 30 s at certain potentials. PS-COOH particles at predetermined concentrations were then added inside the beaker (outside solution) which was in contact with the tip side of the pipette. An Axopatch 200B (Molecular Devices Corporation, CA, USA) was used in voltage-clamp mode to apply a transmembrane potential with a low-pass Bessel filter at 2 kHz bandwidth. The signal was digitized using a Digidata 1440 (Molecular Devices Corporation, CA, USA) at a sampling frequency of 5 kHz. pClamp 10.5 (Molecular Devices Corporation) was used to analyze the data.

The current pulses were characterized by their frequency per unit of time (f) as well as pulse amplitude (Δi) and duration (τ). Δi can be defined as the difference between the values of lowest and initial currents, whereas τ is defined as the time difference between the first drop of current and recovery to the initial value.

Results and discussion

*Characterization of the micro/nanopipettes:*

Characterization of the pipettes were performed by calculating the tip openings directly from SEM and optical images. Fig. 2 shows the SEM images of a nanopipette with 200 nm diameter opening. Optical microscopy images can also be used for calculating the opening diameter of micropipettes. The optical microscopy images for a 7 mm micropipette is given in Fig. 3.

Resistive-pulse sensing of polystyrene particles:

In order to examine the transport properties of PS-COOH particles through the micropipettes, potential and concentra-
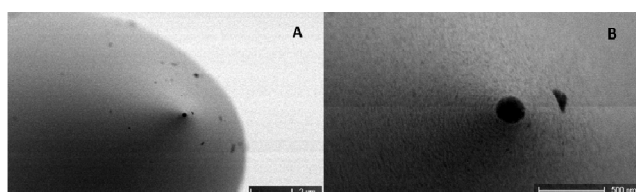

Fig 2. SEM image of a nanopipette (A: x 8K magnification; B: x 50K magnification).
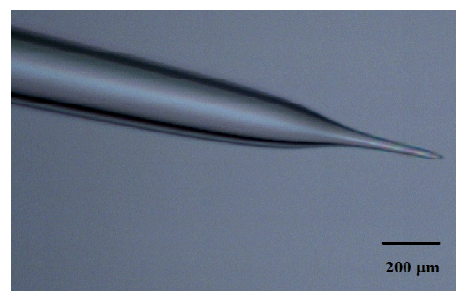
Fig 3. Optical microscopy image of a micropipette (x 20K magnification).

tion dependence of the current-pulses were examined. For this purpose, 7 mm micropipette was used as the PS-COOH particles were 1.05 mm in size. The baseline current was recorded with 10 mM KCl and it was found to be stable, with no current-pulses (events) at 250 mV (Fig. 4A). When the PS-COOH particles (10^8 particles per mL of 10 mM KCl) were introduced to the tip side of the pipette at the same potential, current-pulses were observed (Fig. 4B). The current-pulse signals have shown an upward trend at this potential but as the potential was stepped upwards, the current-pulses first decreased in frequency (Fig. 4C, D, E), then vanished altogether at 360 mV (Fig. 4F). As the potential was further increased, resistive pulses were observed at 400 mV potential (Fig. 4G).

The signal shapes are directly affected by the overall conductance of the pore which is dependent on particle charge, pore surface charge, ionic concentration of the electrolyte solution and the applied electric field. Upward (conductive) signals are encountered when the overall resistance of the pore decreases with the translocation of the particle. These pulses can also be attributed to the particles' (or the surrounding counter-ions') higher conductance than the electrolyte. However as the potential increases, the signals show a downward (resistive) trend, meaning the current pulses are dominated by the volume exclusion effect where translocating particles block the pore and cause drops in the ionic current. This can be attributed to the velocity of the particles. At low potentials the electrophoretic forces that cause the particles to translocate through the pore are low; this means a longer interaction between the particle and pipette tip which can manifest itself as conductive pulses. As the potential increases however, these interactions are no longer possible due to the higher velocity of the particles and the only dominating force on signal shape is volume exclusion effect.
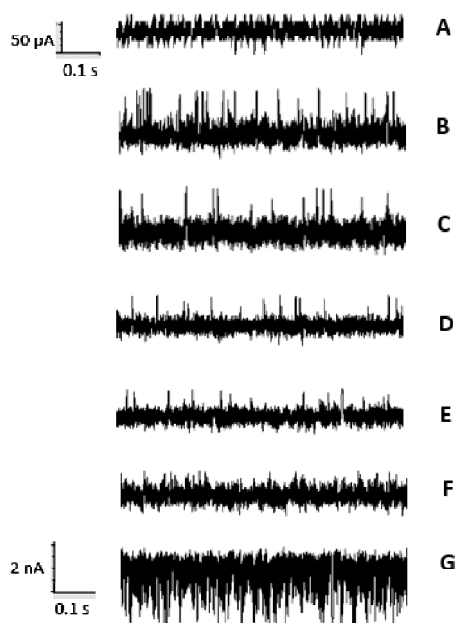
Fig. 4. Current-time traces of 10^8 particle/mL PS-COOH at 250 mV (without analyte) (A), 250 mV (B), 330 mV (C), 340 mV (D), 350 mV (E), 360 mV (F), 400 mV (G).

Effect of PS-COOH concentration was also observed for four different concentration values of 0.5×10^7–10×10^7 number of PS-COOH particles per mL at 300 mV. Fig. 5 shows the linear relationship between current-pulse frequency (f) which is the number of pulses (signals) per second and the concentration of PS-COOH particles (R^2 = 0.957). f was determined by counting the number of pulses in thirty second windows and averaging the counts per second. This finding can be attributed to the increased number of interaction of the analyte and pipette. It is also shown that when the lowest concentration was excluded, R^2 value increased to 0.997. This indicates that a more linear dependence can be observed for higher concentrations.

Verification of the surface modification:

Rectification in the ionic current (or ion current rectification, ICR) can be calculated as the ratio of current values at –1 V and +1 V (eq. (1)). Quartz pipettes have a negative surface charge due to the hydroxyl groups on its surface at neutral pH[20]. Therefore the rectification ratio is expected to be higher than 1. As the surface charge is removed by modification, the I-V curve behavior would change and become more linear. Similarly, if the surface has positive charge, the
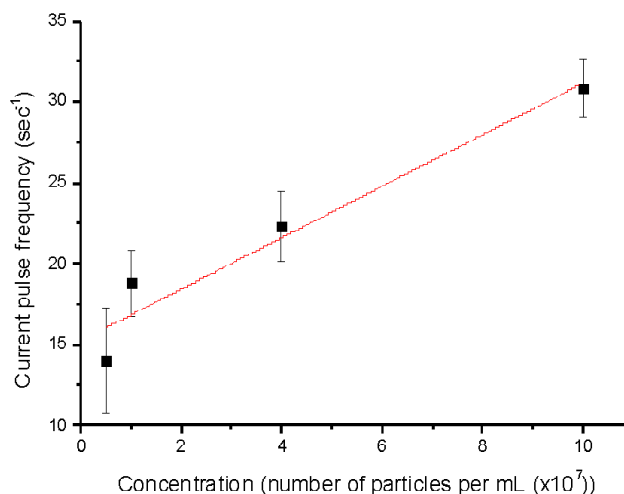
Fig. 5. Effect of PS-COOH concentration on current-pulse frequency (Applied potential = 300 mV).

current rectification would be reversed and the ICR would be lower than 1. So it can be conclude that the I-V curves and ICR provide information about the surface charge of nanopores[20,21].

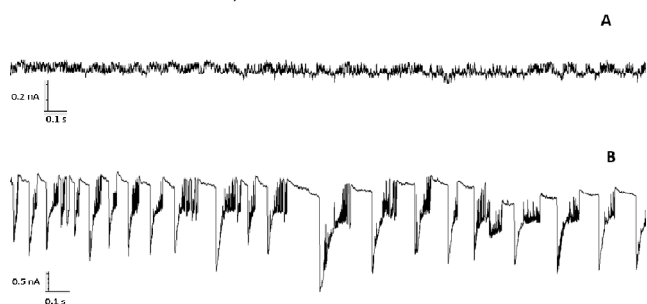$$ICR = \frac{|i_{-1}|}{|i_{+1}|} \tag{1}$$

Fig. 6 shows the I-V curves of bare and modified nanopipette for 10 and 100 mM KCl. ICR values were found to decrease from 1.91 to 0.49 for 10 mM KCl and 3.14 to 0.92 for 100 mM KCl when the surface was modified with APTES. This finding indicates that the surface has indeed gone through modification and the surface charge is relatively more positive for the modified pipette than the bare one.

Resistive-pulse sensing with modified pipettes:

Transport of PS-COOH particles through the modified micropipettes was also carried out. A micropipette with the same size as the bare ones (7 μm) was prepared and modified with APTES. I-t measurements were taken in 30 s periods to evaluate the current-pulses. An important finding was that when bare pipette was used, the threshold voltage where the signals are first observed was found to be 250 mV. Using the modified pipettes, the threshold voltage was as low as 50 mV. Fig. 7 shows the I-t recordings for the translocation of 1×10^7 PS-COOH per mL through bare and modified pipettes in 10 mM KCl at 50 mV potential. The current pulses were also characterized using the scatter plot of pulse amplitudes
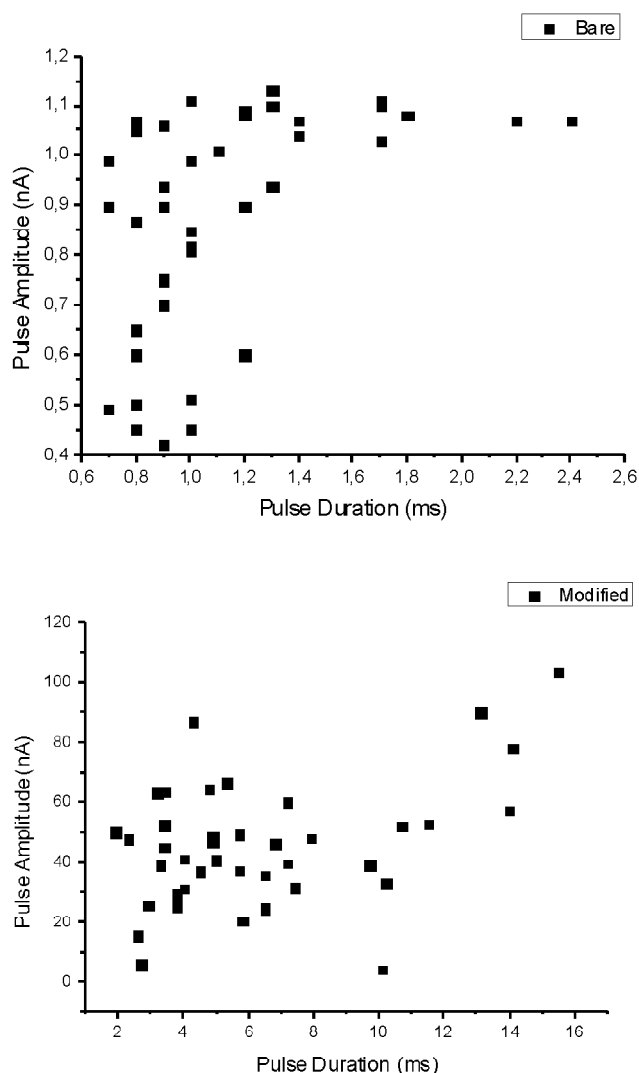
(Δi) vs pulse durations (τ). Scatter plots obtained for 1×10^7 PS-COOH per mL in 10 mM KCl at 300 mV are given in Fig. 8.
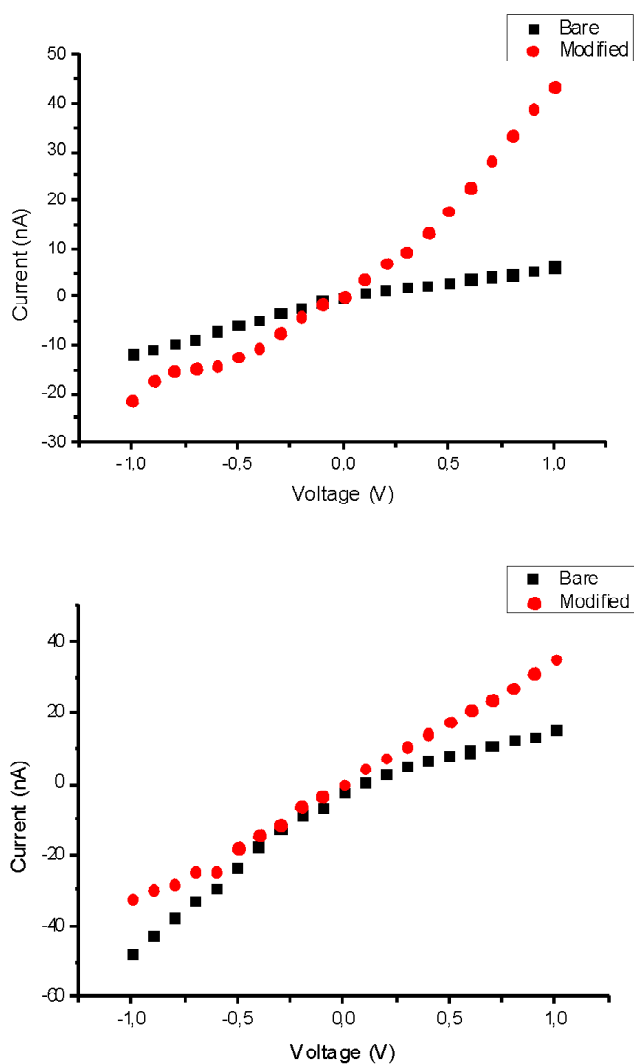
Fig. 6. I-V curves of bare and surface modified pipette (10 mM top, 100 mM bottom).

Fig. 8. Scatter plots of current pulse amplitudes (Δi) vs current pulse durations (τ) obtained from bare pipette (top) and modified pipette (bottom).

The average values of Δi and τ for bare and modified pipettes are given in Table 2 for comparison. It can be concluded from both Fig. 8 and Table 2 that the signal durations are longer and the signal amplitudes are higher for modified pipettes than that of the bare ones. This indicates a better signal to noise ratio and is caused by enhanced interactions of the oppositely charged pipette surface and the particle for

Fig. 7. Current-time (I-t) recording at 50 mV for 1×10^7 PS-COOH per mL in 10 mM KCl using bare pipette (A) and modified pipette (B).

Table 2. Average current-pulse amplitude and current-pulse duration values for bare and modified pipettes

	τ (ms)	Δi (nA)
Bare	1.14±0.40	0.88±0.22
Modified	6.35±3.58	45.65±21.15

the modified pipette. A six-fold difference was obtained for current pulse duration values whereas the current pulse amplitudes were almost fifty times higher for modified pipettes.

Conclusions

In this work micro/nanopipettes were prepared by pulling from quartz capillaries. Sensing of 1.05 μm diameter PS-COOH was shown using the prepared micropipettes. Translocation of the particles were studied for a variety of potential and concentration values. It was shown that the applied potential had a significant effect on the signal shape. Lower potentials (i.e. 250 mV) generated upward (conductive) signals whereas downward (resistive) signals were obtained when the potential was increased (i.e. 400 mV) where volume exclusion effect was dominating. Increasing the concentration of the PS-COOH particles has caused a linear increase on the number of signals. Inner surface of the prepared pipettes were modified with APTES using silane chemistry. The modification was verified by showing the decrease in ionic current rectification on the I-V curves of bare and modified nanopipettes. In order to compare the performance of bare and modified pipettes, the translocation of the analyte was also performed using modified pipettes. It was shown that much lower potentials were applicable for modified pipettes than bare ones. Furthermore the current pulse durations were longer for modified pipettes and the current pulse amplitudes were higher. An enhanced sensing of PS-COOH particles was shown by applying the verified method for the surface modification on micropipettes and taking advantage of the neutral/positive surface charge of these pipettes. Future work includes simultaneous separation of charged molecules using synthetic porous structures (pipettes, polymers etc.) and exploring nanopipette geometries for resistive-pulse sensing.

References

1. T. Vaclavek, J. Prikryl and F. Foret, *J. Sep. Sci.*, 2018, **42(1)**, 445.

2. H. Zhang, C. H. Chon, X. Pan and D. Li, *Microfluid. Nanofluid.*, 2009, **7(6)**, 739.

3. S. Umehara, N. Pourmand, C. D. Webb, R. W. Davis, K. Yasuda and M. Karhanek, *Nano Lett.*, 2006, **6(11)**, 2486.

4. C. Dekker, *Nat. Nanotechnol.*, 2007, **2(4)**, 209.

5. (a) D. Kaya, A. Dinler, N. San and K. Kececi, *Electrochim. Acta*, 2016, **202**, 157; (b) D. Fologea, E. Brandin, J. Uplinger, D. Branton and J. Li, *Electrophoresis*, 2007, **28(18)**, 3186; (c) S. R. Park, H. Peng and X. S. Ling, *Small*, 2007, **3(1)**, 116.

6. R. Spohr, C. Zet, B. E. Fischer, H. Kiesewetter, P. Apel, I. Gunko, T. Ohgai and L. Westerberg, *Nucl. Instrum. Meth. B*, 2010, **268(6)**, 676.

7. (a) K. K. Hu, Y. X. Wang, H. J. Cai, M. V. Mirkin, Y. Gao, G. Friedman and Y. Gogotsi, *Anal. Chem.*, 2014, **86(18)**, 8897; (b) X. Q. Gong, A. V. Patil, A. P. Ivanov, Q. Y. Kong, T. Gibb, F. Dogan, A. J. deMello and J. B. Edel, *Anal. Chem.*, 2014, **86(1)**, 835.

8. C. B. Rosen, D. Rodriguez-Larrea and H. Bayley, *Nat. Biotechnol.*, 2014, **32(2)**, 179.

9. D. Kaya and K. Kececi, *Bulg. Chem. Commun.*, 2017, **49**, 37.

10. (a) K. Kececi, L. T. Sexton, F. Buyukserin and C. R. Martin, *Nanomedicine-UK*, 2008, **3(6)**, 787; (b) P. Chen, J. J. Gu, E. Brandin, Y. R. Kim, Q. Wang and D. Branton, *Nano Lett.*, 2004, **4(11)**, 2293; (c) G. F. Schneider and C. Dekker, *Nat. Biotechnol.*, 2012, **30(4)**, 326.

11. Y. X. Wang, K. Kececi, M. V. Mirkin, V. Mani, N. Sardesai and J. F. Rusling, *Chem. Sci.*, 2013, **4(2)**, 655.

12. (a) Y. Yu, J.-M. Noël, M. V. Mirkin, Y. Gao, O. Mashtalir, G. Friedman and Y. Gogotsi, *Anal. Chem.*, 2014, **86(7)**, 3365; (b) M. Karhanek, J. T. Kemp, N. Pourmand, R. W. Davis and C. D. Webb, *Nano Lett.*, 2005, **5(2)**, 403; (c) B. Kim, T. Murray and H. Bau, *Nanotechnol.*, 2005, **16(8)**, 1317.

13. K. Kececi, N. San and D. Kaya, *Talanta*, 2015, **144**, 268.

14. Z. S. Siwy, *Adv. Funct. Mater.*, 2006, **16(6)**, 735.

15. (a) R. Proksch, R. Lal, P. K. Hansma, D. Morse and G. Stucky, *Biophys. J.*, 1996, **71(4)**, 2155; (b) K. T. Rodolfa, A. Bruckbauer, D. Zhou, Y. E. Korchev and D. Klenerman, *Angew. Chem. Int. Ed.*, 2005, **44(42)**, 6854; (c) S. An, C. Stambaugh, G. Kim, M. Lee, Y. Kim, K. Lee and W. Jhe, *Nanoscale*, 2012, **4(20)**, 6493.

16. C. Kranz, *Analyst*, 2014, **139(2)**, 336.

17. C. A. Morris, A. K. Friedman and L. A. Baker, *Analyst*, 2010, **135(9)**, 2190.

18. Y. Fu, H. Tokuhisa and L. A. Baker, *Chem. Commun.*, 2009, **(32)**, 4877.

19. N. Sa, Y. Fu and L. A. Baker, *Anal. Chem.*, 2010, **82(24)**, 9963.

20. C. Wei, A. J. Bard and S. W. Feldberg, *Anal. Chem.*, 1997, **69(22)**, 4627.

21. Z. Siwy, E. Heins, C. C. Harrell, P. Kohli and C. R. Martin, *J. Am. Chem. Soc.*, 2004, **126(35)**, 10850.